International Journal of Nanomedicine

Dovepress
open access to scientific and medical research

Open Access Full Text Article

ORIGINAL RESEARCH

Influence of nanotopography on periodontal ligament stem cell functions and cell sheet based periodontal regeneration

This article was published in the following Dove Press journal:
International Journal of Nanomedicine
19 June 2015
Number of times this article has been viewed

Hui Gao[1–3,*]
Bei Li[1,2,*]
Lingzhou Zhao[4]
Yan Jin[1,2]

[1]State Key Laboratory of Military Stomatology, Center for Tissue Engineering, School of Stomatology, The Fourth Military Medical University, [2]Research and Development Center for Tissue Engineering, The Fourth Military Medical University, Xi'an, Shaanxi, [3]Department of Stomatology, PLA 309th Hospital, Beijing, [4]State Key Laboratory of Military Stomatology, Department of Periodontology, School of Stomatology, Fourth Military Medical University, Xi'an, Shaanxi, People's Republic of China

*These authors contributed equally to this work

Abstract: Periodontal regeneration is an important part of regenerative medicine, with great clinical significance; however, the effects of nanotopography on the functions of periodontal ligament (PDL) stem cells (PDLSCs) and on PDLSC sheet based periodontal regeneration have never been explored. Titania nanotubes (NTs) layered on titanium (Ti) provide a good platform to study this. In the current study, the influence of NTs of different tube size on the functions of PDLSCs was observed. Afterward, an ectopic implantation model using a Ti/cell sheets/hydroxyapatite (HA) complex was applied to study the effect of the NTs on cell sheet based periodontal regeneration. The NTs were able to enhance the initial PDLSC adhesion and spread, as well as collagen secretion. With the Ti/cell sheets/HA complex model, it was demonstrated that the PDLSC sheets were capable of regenerating the PDL tissue, when combined with bone marrow mesenchymal stem cell (BMSC) sheets and HA, without the need for extra soluble chemical cues. Simultaneously, the NTs improved the periodontal regeneration result of the ectopically implanted Ti/cell sheets/HA complex, giving rise to functionally aligned collagen fiber bundles. Specifically, much denser collagen fibers, with abundant blood vessels as well as cementum-like tissue on the Ti surface, which well-resembled the structure of natural PDL, were observed in the NT5 and NT10 sample groups. Our study provides the first evidence that the nanotopographical cues obviously influence the functions of PDLSCs and improve the PDLSC sheet based periodontal regeneration size dependently, which provides new insight to the periodontal regeneration. The Ti/cell sheets/HA complex may constitute a good model to predict the effect of biomaterials on periodontal regeneration.

Keywords: titanium implant, titania nanotubes, periodontal ligament stem cells, periodontal regeneration, cell sheets

Introduction

Periodontal regeneration is of great clinical significance.[1] The periodontal tissues, including alveolar bone, periodontal ligament (PDL), and root cementum, play an important role to support the normal function of a tooth. Unfortunately, a common and widespread disease, periodontitis, can cause the destruction of the periodontal tissues and subsequent tooth loss, if untreated.[2] Besides controlling the inflammation status and progression of periodontitis, the ultimate goal of periodontal therapy is to restore impaired periodontal tissues to their original architecture. Though various regenerative therapies, such as guided tissue regeneration, have been routinely utilized in clinical practice, the outcomes are limited, with poor clinical predictability.[3] Stem cell–based tissue engineering is believed to be a promising approach to generate more predictable and efficient periodontal tissue restoration.[4] Tissue-engineered tooth regeneration is believed to be a more ideal approach for missing tooth restoration, and successful periodontal tissue regeneration is an essential part of this.[5,6] For successful tissue-engineered tooth regeneration, use

Correspondence: Yan Jin
State Key Laboratory of Military Stomatology, Center for Tissue Engineering, School of Stomatology, The Fourth Military Medical University, Number 145 West Changle Road, Xincheng District, Xi'an 710032, Shaanxi, People's Republic of China
Tel +86 29 8477 6147
Fax +86 29 8321 8039
Email yanjin@fmmu.edu.cn

Lingzhou Zhao
State Key Laboratory of Military Stomatology, Department of Periodontology, School of Stomatology, The Fourth Military Medical University, Number 145 West Changle Road, Xincheng District, Xi'an 710032, Shaanxi, People's Republic of China
Tel +86 29 8477 6093
Fax +86 29 8477 6096
Email zhaolingzhou1983@hotmail.com

of a dental implant is, currently, the most ideal choice for the missing tooth restoration. Generally, direct bone-to-implant contact, defined as "osseointegration", is considered as the optimal healing response for a dental implant.[7] Though a high success rate has been accomplished, this rigid ankylotic anchorage of dental implants to jawbone brings many issues, of which the most outstanding is the adjacent bone adsorption due to the absence of a cushion mechanism.[8,9] The formation of a PDL-like tissue around an implant should improve its performance. Thus, successful periodontal regeneration provides a promising approach to achieve the ultimate purpose of periodontal therapy and to further augment the performance of the dental implant, and constitutes an essential part of accomplishing whole tooth regeneration.

Since the successful isolation of stem cells from human PDL, termed "PDL stem cells" (PDLSCs), by Seo et al[10] these have constituted a good choice for stem cell–based periodontal regeneration.[10,11] It has been shown that in combination with a suitable scaffold, PDLSCs can regenerate a cementum/PDL-like structure in vivo.[10,11] Specifically, cell sheet technology, which can generate high-density cells with abundant endogenous deposited extracellular matrix (ECM) and intact cell-to-cell contact, has been applied for periodontal regeneration.[11,12] After transplantation of the PDLSC sheets to a periodontal defect model, significant periodontal regeneration has been observed, with both newly formed cementum and well-oriented PDL fibers.[12] It will be meaningful to well manipulate the functions of PDLSCs to achieve more satisfactory periodontal regenerative results.

The fact that the shape and differentiation of mesenchymal stem cells (MSCs) can be driven by the material/cell interface suggests a unique strategy to manipulate the stem cell fate, instead of reliance on complex soluble chemical cues. For example, topographical cues, especially nanoscale ones, are observed to control the functions of stem cells.[13] One impressive study from Dalby et al[13] demonstrated that slightly disordered nanopits, with a diameter of 120 nm, layered on polymethylmethacrylate were able to induce human MSC osteogenic differentiation. A later paper from the same group, reported by McMurray et al displayed that absolutely ordered nanopits of the same diameter retained the stem cell phenotype and maintained stem cell growth of MSCs over 8 weeks.[14] Titania nanotubular topography constitutes another excellent example and has been widely documented to be a powerful modulator of cell shape, adhesion, proliferation, and differentiation.[15–19] Nonetheless, whether the functions of PDLSCs can be modulated by the nanotopography has never been reported.

Easily fabricated titania nanotubes (NTs) layered on titanium (Ti) with finely tunable tube size, constitute an excellent platform to explore the effect of nanotopography on cell functions. Here, the influence of NTs of different tube size on the in vitro functions of PDLSCs was systemically observed. Furthermore, the effects of NTs on PDLSC sheet based periodontal regeneration were assessed by applying a specific sandwich-like model that was designed in light of the natural structure of the cementum–PDL–alveolar bone complex. In this model, the Ti rod was wrapped by two sheets of PDLSC, then one sheet of bone marrow MSC (BMSC), and finally surrounded by a hydroxyapatite (HA) block, where the PDLSC sheets were intended to regenerate the cementum and PDL-like tissues, and the BMSC sheet was supposed to form the bone tissue. The study provides a novel insight on the potential effect of the nanotopography on PDLSC function and periodontal regeneration.

Materials and methods

Specimen preparation

Pure Ti plates (10×10×1 mm^3) as well as Ti rods (Φ 3×5 mm^3) (99.9%) (Northwest Institute for Nonferrous Metal Research, Xi'an, People's Republic of China) were used for cellular and animal studies, respectively. After polishing with SiC sandpaper, from 400 to 1,500 grit, and ultrasonic cleaning, the samples were anodized in an electrolyte containing 0.5 wt% hydrofluoric acid and 1 M phosphoric acid for 1 hour, with a direct current (DC) power supply and a platinum cathode at 5, 10, and 20 V, respectively, to fabricate the NTs of different tube size, designated as NT5, NT10, and NT20. The polished flat Ti samples were used as a control. The morphology of the samples was inspected by field-emission (FE) scanning electron microscopy (SEM) (FE-SEM) (S-4800; Hitachi Ltd., Tokyo, Japan). The samples were sterilized with cobalt-60 before the cell plating and animal studies.

Cell culture

The experimental protocols were approved by the ethics committee (Institutional Review Board for Human Subjects Research) of the School of Stomatology, Fourth Military Medical University. All donors provided written informed consent for the donation of their removed teeth and bone chips for this research project. Following the informed consent, six impacted third molars with healthy PDL tissue were obtained from six donors of 18–28 years. Jaw bone chips were also harvested from the same six donors because bone-removing surgery was required during the extraction of their impacted third molars.

The PDL was gently separated from the tooth root surface and then digested in a solution containing 3 mg/mL collagenase type I (Sigma-Aldrich Corp, St Louis, MO, USA)

and 4 mg/mL dispase (Sigma-Aldrich Corp) for 1 hour at 37°C. The tissue explants were then plated into six-well culture dishes (Costar®; Corning Inc, Corning, NY, USA) and cultured with basal medium containing α modified minimum essential medium (α-MEM) (Hyclone®; Thermo Fisher Scientific Inc, Waltham, MA, USA) supplemented with 10% fetal bovine serum (FBS) (Hyclone), 0.292 mg/mL glutamine (Hyclone), and 100 units/mL penicillin streptomycin (Hyclone), and finally, incubated at 37°C in a humidified atmosphere with 5% CO_2.

For the jaw bone MSC culture, the obtained bone chips were aseptically rinsed twice in phosphate-buffered saline (PBS), and then the bone marrow contents were flushed out from the bone marrow cavity with α-MEM. The resultant medium was centrifuged at 1,000 rpm for 5 minutes. Finally, the cells were resuspended with α-MEM and cultured in six-well plates. After 3 days, the floating cells were removed, and the adherent cells were cultured to approach confluence.

To further purify the stem cells, single-cell suspensions of the primary cells were cloned using the limiting dilution technique. All colonies were then pooled and expanded. To avoid cell behavioral changes that are associated with prolonged culture, the cells at passages 2–4 (P2–P4) were used in the present study.

Characterization of the PDLSCs and BMSCs

Colony-forming unit-fibroblast (CFU-F) assays

The PDLSCs or BMSCs (P3) (1×10^3 cells) were cultured in 10 cm–diameter culture dishes (Corning Inc) for CFU-F assays. Aggregates with more than 50 cells viewed under the microscope were counted as a colony. The experiment was repeated at least three times.

In vitro multiple differentiation potentials of the PDLSCs and BMSCs

The PDLSCs or BMSCs (P3) (2×10^5 cells) were cultured in six-well plates with the basal medium. At confluence, the medium was shifted to osteogenic medium (basal medium supplemented with 50 μg/mL L-ascorbic-2-phosphate [MP Biomedicals, Santa Ana, CA, USA]), 0.1 mM dexamethasone, and 5 mM β-glycerophosphate [Sigma-Aldrich Corp]), or adipogenic medium (basal medium supplemented with 1 μM dexamethasone, 10 μM insulin, 0.5 mM 1-methyl-3-isobutylxanthine, and 200 μM indomethacin [all from Sigma-Aldrich Corp]). The induction medium was refreshed every 3 days. After 3-week adipogenic induction, the cells were fixed with 4% paraformaldehyde and stained with 0.3% Oil Red O (Sigma-Aldrich Corp), and then lipid droplets were identified microscopically. After a 4-week osteogenic induction, the cells were fixed with 4% paraformaldehyde and stained with 2% Alizarin Red S (pH 4.2) (Kermel, Colmar, France). After removing the unbound and nonspecifically bound stain by copious rinsing with distilled water, stained calcium nodules were identified microscopically.

Flow cytometry (FCM) analysis

To characterize the immunophenotype of in vitro–expanded PDLSCs and BMSCs, FCM analysis was conducted to measure the expression of MSC- and non-MSC-associated surface markers at early passages (P2). Briefly, the adherent cells were washed twice with PBS and liberated by 2 mL of 0.05% trypsin (Sigma-Aldrich Corp). Then, the single-cell suspension was washed twice and resuspended in PBS containing 3% FBS. For the identification of the MSC phenotype, approximately 5×10^5 PDLSCs/ or BMSCs/200 μL of PBS in each EP tube were incubated with phycoerythrin- or fluorescein isothiocyanate–conjugated monoclonal antibodies for human CD31, CD44, CD105 (eBioscience, San Diego, CA, USA), CD34, CD40, CD146, STRO-1, and CD45 (BioLegend, San Diego, CA, USA) for 1 hour at 4°C in the dark. The wells without any antibodies were used as negative control. Then, the cells were washed twice with 1 mL PBS. Finally, the labeled cells were analyzed by FCM (Becton Coulter Inc, Brea, CA, USA).

Initial adherent number of the PDLSCs on the Ti samples

The PDLSCs were seeded on the Ti samples placed in 24-well plates, at a density of 1×10^4 cells/well. After culturing for 0.5, 1, and 2 hours, the adherent cells were fixed and stained with 4′,6′-diamidino-2-phenylindole (DAPI) (Sigma-Aldrich Corp). The cell numbers in each sample were counted in three random 5+ fields, under an epifluorescence microscope (Leica Microsystems, Wetzlar, Germany).

Proliferation and cell cycle analysis of the PDLSCs seeded on the Ti samples

The PDLSCs were seeded on the samples placed in 24-well plates at a density of 1×10^4 cells/well. After culturing for 1, 3, 5, and 7 days, cell proliferation was assessed using a CCK-8 assay. In brief, at the prescribed time points, the samples were rinsed with PBS and transferred to new 24-well plates. Then 300 mL α-MEM and 30 mL CCK-8 solution (Beyotime Institute of Biotechnology, Shanghai, People's Republic of China) were added to each well and incubated at 37°C for 2 hours. Finally, the absorbance was measured at 450 nm.

The PDLSCs were inoculated on the samples at a density of 1×10^4 cells/well. After 3 and 5 days of culture, the cells on six samples for each group were trypsinized and pooled for cell cycle analysis. After washing with PBS, the cells were resuspended in 1 mL of PBS with repeated vibration to get a suspension. The cells in the suspension were fixed with ice-cold dehydrated ethanol overnight at 4°C. The fixed cells were washed twice with PBS and stained with 100 mg/mL propidium iodide (PI) (Sigma-Aldrich Corp) at 4°C for 30 minutes. The PI-elicited fluorescence of individual cells was measured using FCM. At least 40,000 cells were analyzed for each sample. The amounts of cells residing in the G0/G1 phase, S phase, and G2/M phase were determined.

Morphology of the PDLSCs on the Ti samples

The PDLSCs were seeded at a density of 5×10^3 cells/well. After 2 and 6 hours, as well as after 1 and 2 days of incubation, the samples, with attached cells, were washed with PBS, fixed in 3% glutaraldehyde, dehydrated in a graded ethanol series, freeze-dried, and sputter coated with gold prior to observation by FE-SEM.

Collagen secretion by the PDLSCs on the Ti samples

PDLSCs (1×10^4) were added onto each specimen placed in the 24-well plates and cultured for 14, 21, and 28 days in the absence and presence of osteogenic supplements. The collagen secretion ability of the cells was evaluated by Sirius Red staining as previously reported.[18,20]

Alkaline phosphatase (ALP) produced by the PDLSCs on the Ti samples

A cell suspension of 1 mL was seeded on each sample at a density of 1×10^4 cells/mL. After culturing for 7 and 14 days in the absence and presence of osteogenic supplements, the cells were washed and fixed. ALP staining was conducted with an ALP color development kit (Beyotime Institute of Biotechnology), and ALP activity was determined by an ALP activity detection kit (Jiancheng Bioengineering Institute, Nanjing, People's Republic of China), according to the manufacturer's suggested protocols.

Mineralized ECM nodule formation by the PDLSCs on the Ti samples

PDLSCs (1×10^4) were added to each Ti sample that was already placed in the 24-well plates and cultured for 28 days in the absence and presence of osteogenic supplements. After washing and fixation, the cells were stained with 1 wt% Alizarin Red S (pH 4.2) (Kermel) for 3 minutes to display the mineralized ECM nodule formation. The stained mineralized nodules were then identified microscopically. The relative nodule area was calculated from at least three randomly selected fields from each specimen, using ImageJ software.

Gene expression by the PDLSCs cultured on the Ti samples, as well as the in vitro cultured Ti/cell sheets/HA complexes

The cells were seeded at a density of 1×10^4 cells/well and cultured for 1 and 2 weeks, and were then harvested using TRIzol (Gibco®; Life Technologies Corp, Carlsbad, CA, USA) to extract the RNA. The PDLSCs and BMSCs of passage 3 were used to prepare the cell sheets according to the methods described in the literature.[21] PDLSCs or BMSCs, at a density of 1×10^6 cells/well, were plated into six-well plates and cultured until 100% confluence. Then the cell culture medium was shifted to the cell sheet–inducing medium (α-MEM supplemented with 10% FBS, 1% penicillin and streptomycin, and 50 mg/mL vitamin C). After 6–10 days of culture, the cell sheets initially formed. The cell sheets obtained were about 35 mm in diameter. To prepare the Ti/cell sheets/HA complex, the Ti rods were wrapped with two PDLSC sheets, then a single BMSC sheet, and finally, HA block. The Ti/cell sheets/HA complexes were cultured in the 12-well plate for 1 month and then harvested using TRIzol to extract the RNA. An equivalent amount of RNA from each sample was reverse transcribed into complementary DNA (cDNA) using a Superscript II first-strand cDNA synthesis kit (Invitrogen®; Life Technologies Corp). The real-time quantitative reverse-transcription polymerase chain reaction (qRT-PCR) analysis on the genes, including *S100A4*, *POSTN*, *COL-I*, and *COL-III* was performed on the Applied Biosystems 7500 using the QuantiTect® Sybr® Green Kit (Qiagen, Venlo, the Netherlands). The primers for the target genes were listed in Table 1. The expression levels of the target genes were normalized to that of the housekeeping gene *β-actin*.

In vivo ectopic implantation of the Ti/cell sheets/HA complex

The Ti/cell sheets/HA complexes were then implanted subcutaneously into the dorsal surface of 6-week-old immunocompromised mice (Animal Center of the Fourth Military Medical University, Xi'an, People's Republic of China). The mice were maintained in pathogen-free conditions at 26°C, at 70% relative humidity, and under a 12-hour light/dark cycle. All animal procedures used in this study were approved by the research ethics committee of The Fourth

Table 1 The list of the target genes and the primer sequences used for qRT-PCR

Gene	Forward primer sequence (5′-3′)	Reverse primer sequence (5′-3′)
COL-I	AGACGAAGACATCCCACCAATC	GATCACGTCATCGCACAACAC
COL-III	ACAGCCTCCAACTGCTCCTAC	GATAGCCTGCGAGTCCTCCT
POSTN	GCTGCCATCACATCGGACATA	GCTCCTCCCATAATAGACTCAGAACA
S100A4	TCGGGCAAAGAGGGTGACA	TGGCGATGCAGGACAGGA
β-actin	TGGCACCCAGCACAATGAA	CTAAGTCATAGTCCGCCTAGAAGCA

Abbreviation: qRT-PCR, quantitative reverse-transcription polymerase chain reaction.

Military Medical University. There were four animals in each sample group. At 8 weeks after implantation, the mice were euthanized, and the implanted samples were harvested, fixed in 4% neutral formaldehyde (Sigma-Aldrich Corp), embedded in resin, and sectioned. The sections were stained with the Van Gieson staining, and hard-tissue histological analyses were performed using light microscopy.

Statistical analysis

All biological experiments were performed thrice with quadruplicates in each experiment. Representative results from one independent experiment were depicted in this report. One-way analysis of variance (ANOVA) and Student–Newman–Keuls post hoc tests were used to determine the level of significance. Statistical significance was considered at $P<0.05$, 0.01, and 0.001.

Results

The SEM characterization of the NTs

The morphology of the fabricated samples was characterized by the FE-SEM (Figure 1). The anodized Ti samples had evenly distributed NTs. The images show highly ordered, vertically aligned NTs, with three different tube sizes between 25 and 90 nm, created by controlling the anodization potentials from 5 to 20 V. The tube size, the tube wall width, and the intertubular distance all increased with the increasing anodization potential. The NTs on NT5 had an average diameter of about 25 nm and a tube wall width of 5 nm. In particular, the NTs on NT5 were in close proximity to each other with almost no intertubular space. The NTs on NT10 had an average diameter of about 50 nm, a tube wall width of 10 nm, and an intertubular distance of 15–20 nm. The NTs in NT20 had an average diameter of about 90 nm, a tube wall width of 15 nm, and an intertubular distance of 25–30 nm. The NTs of different size provided a good platform to study the effect of nanosize on PDLSC function as well as on cell sheet based PDL regeneration.

Colony-forming ability, multiple differentiation potentials, and surface markers of the PDLSCs and BMSCs

To identify the self-renewal potential of PDLSCs and BMSCs, the ability of CFU-F formation was determined (Figures S1A and S2A). The cells assumed a spindle-shape, and single colonies formed 12 days after being plated at a low density, confirming the CFU-forming capacity of the PDLSCs and BMSCs. With suitable inducers, PDLSCs and BMSCs can accumulate lipid droplets within the cytoplasm, as was confirmed by Oil Red O staining (Figures S1C and S2C), or form mineralized ECM, as was shown by staining with Alizarin Red S (Figures S1B and S2B). The PDLSCs and BMSCs positively expressed MSC markers, including CD44, CD105, CD146, and STRO-1, but were negative for hematopoietic lineage markers, including CD34 and CD45, and platelet endothelial cell makers CD31and CD40 (Figures S1D and S2D).

The initial adherent number of the PDLSCs on the Ti samples

Initial cell adhesion to the biomaterial surface is considered to be one of the most key events for a good cell/biomaterial

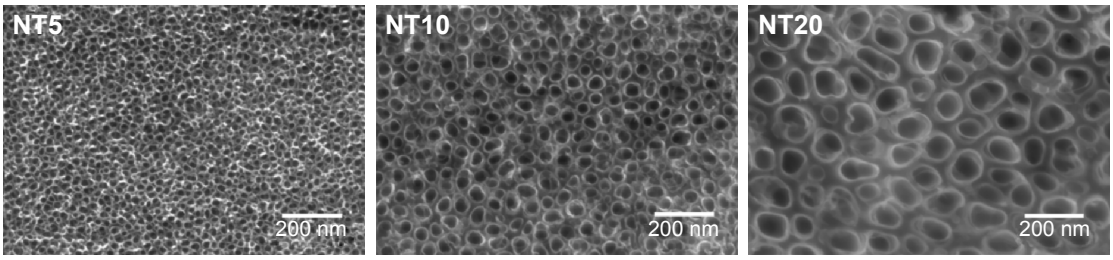

Figure 1 FE-SEM images of NT5, NT10, and NT20.
Note: Scale bars are 200 nm.
Abbreviations: FE-SEM, field-emission scanning electron microscopy; NT, nanotube.

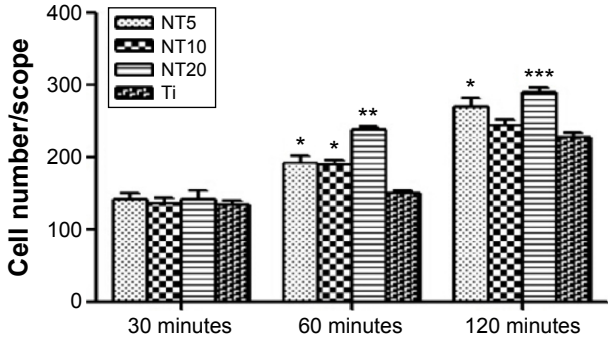

Figure 2 The PDLSC adhesion measured by counting the DAPI-stained cells under a fluorescence microscope after 30, 60, and 120 minutes of incubation.
Notes: *$P<0.05$, **$P<0.01$, and ***$P<0.001$ compared with the Ti control.
Abbreviations: DAPI, 4′,6′-diamidino-2-phenylindole; NT, nanotube; PDLSC, periodontal ligament stem cell; Ti, titanium.

interaction. The influence of the NTs on the initial cell adhesion was displayed by DAPI-staining (Figures 2 and S3). At 30 minutes, there was no obvious difference in the adherent cell number on the different Ti samples. At 60 and 120 minutes, the adherent cell numbers on the NTs were larger than those on the Ti control surface. Among the three nanotubular surfaces, NT20 generated the highest initial adherent cell number at 60 and 120 minutes but without statistical significance.

The cell cycle analysis and proliferation of the PDLSCs on the Ti samples

The influence of the NTs on the cell cycle propagation of PDLSCs was also monitored (Figure 3A). At day 3, there was no obvious difference in the percentage of S+G2M phases among different groups (10.38%, 11.02%, 12.25%, and 11.36% for NT5, NT10, NT20, and the Ti control, respectively). At day 5, NT5 and NT10 induced slightly higher percentages of S+G2M phases (18.55% and 19.71%, respectively) compared with the Ti control (10.72%), but NT20 induced no obvious difference (11.81%).

Cell proliferation was measured using a CCK-8 assay (Figure 3B). Generally, the PDLSCs grew well on all the Ti samples, showing a time-dependent growth pattern, with incubation time from 1 to 7 days. At day 1, the PDLSC numbers on the NTs were slightly smaller than those on the Ti control. At days 3, 5, and 7, the PDLSC numbers on NT10 and NT20 were similar to those on the Ti control, while NT5 induced an obviously lower cell proliferation than did the Ti control.

The morphology of the PDLSCs on the Ti samples

Figures 4 and 5 exhibit the morphology of the adherent PDLSCs on the Ti samples at the earlier stage of 2 and 6 hours and the later stage of 1 and 2 days, during the cell/biomaterial interaction. As shown in Figure 4, from 2 to 6 hours, the cell morphology shifted from an initially round, poorly spread cell shape with relatively short protrusions to a well-extended spindle one with abundant long lamellipodia, on all the Ti samples. At 2 hours, an obvious phenomenon was that the NTs induced a quicker cell spread process than did the Ti control. The cells on NT5, NT10, and NT20 showed an obviously larger cell area with more cell protrusions than did those on the Ti control. The higher-magnification pictures display that the cells on the NTs had many filopodia, while those on the Ti control did not. At 6 hours, there was no obviously discernible morphological difference between the cells on the different Ti samples. After as long as 1 and 2 days of culture, the same trends – that the cells on the NTs spread better and showed more and longer lamellipodia and filopodia than did those on the Ti control – were still obviously observed.

The collagen secretion of the PDLSCs on the Ti samples

The collagen-secretion ability of the PDLSCs was assessed after 14, 21, and 28 days of incubation in the absence and presence of osteogenic supplements, by Sirius Red staining (Figure 6). The optical images demonstrated that the PDLSCs were able to synthesize and secrete certain amounts of collagen on all the Ti samples and that the secreted collagen amounts increased with the culture time from 14 to 21 days. At day 14, similar trends for the collagen secretion amounts of the different Ti samples were observed in the absence and presence of osteogenic supplements. The NTs gave rise to more collagen secretion than did the Ti control ($P<0.05$ for NT5 and NT10). After 21 days of culture, in the absence of osteogenic supplements, a similar trend to that at day 14 was witnessed ($P<0.05$). While in the presence of osteogenic supplements, similar secreted collagen amounts were found on the Ti samples except for NT10, which generated a much higher amount ($P<0.05$). At as long as 28 days of incubation, in the absence of osteogenic supplements, similar secreted collagen amounts were found on the different Ti samples except for NT10, which generated a higher amount ($P<0.05$), and in the presence of osteogenic supplements, there was no obvious difference in the collagen-secretion among the different Ti samples.

The ALP staining and activity of the PDLSCs on the Ti samples

The ALP product, in the absence and presence of osteogenic supplements, was presented in Figure 7. From the ALP

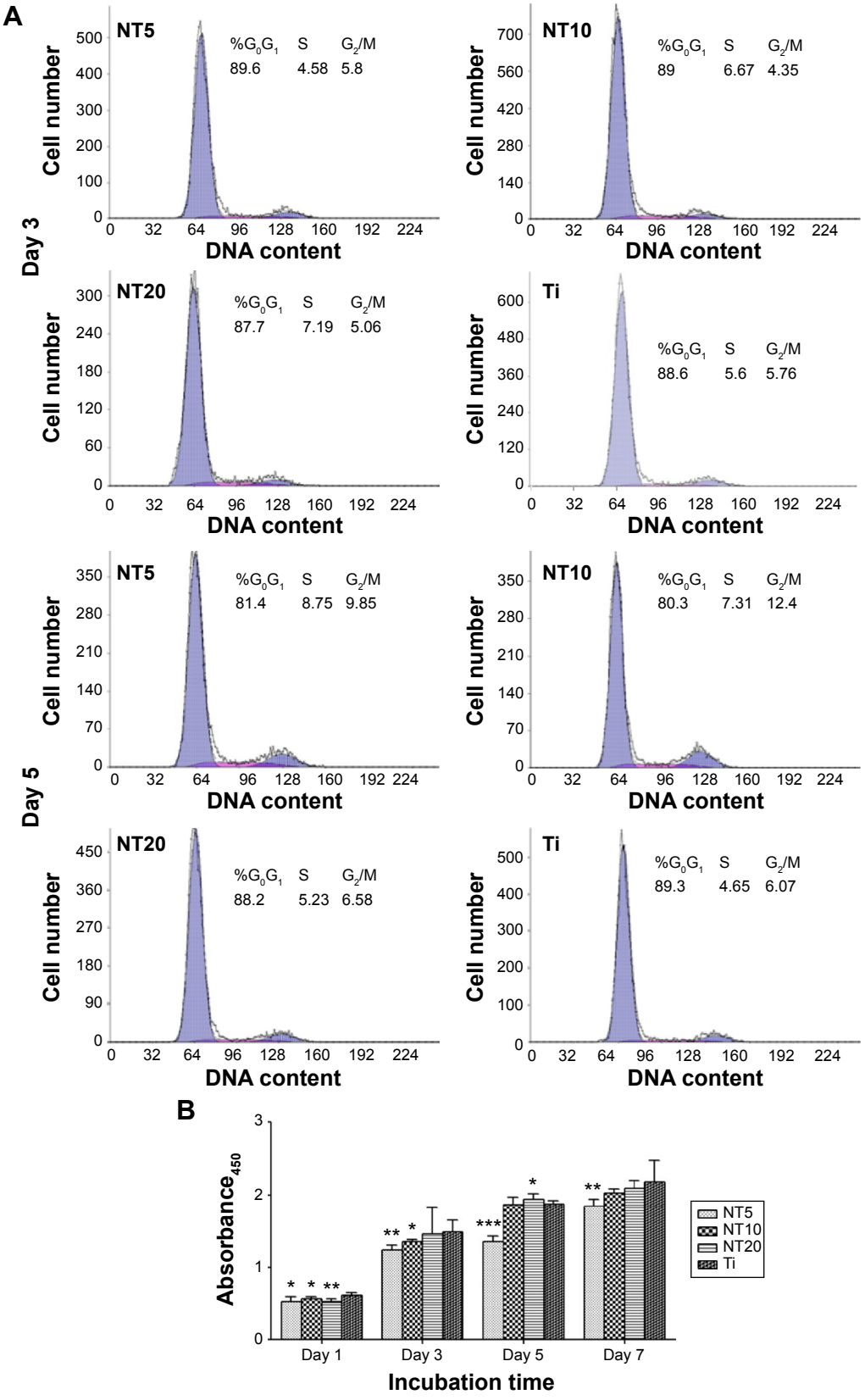

Figure 3 (**A**) Representative cell cycle distribution graphs of PDLSCs cultured on different samples for 3 and 5 days, which were determined by FCM. The percentages of cells residing in the G_0/G_1 phase, S phase, and G_2/M phase are shown in the graphs. (**B**) Cell proliferation measured by the CCK-8 assay after culturing the PDLSCs on the different samples for 1, 3, 5, and 7 days.

Notes: *$P<0.05$, **$P<0.01$, and ***$P<0.001$ compared with the Ti control.

Abbreviations: FCM, flow cytometry; NT, nanotube; PDLSC, periodontal ligament stem cell; Ti, titanium.

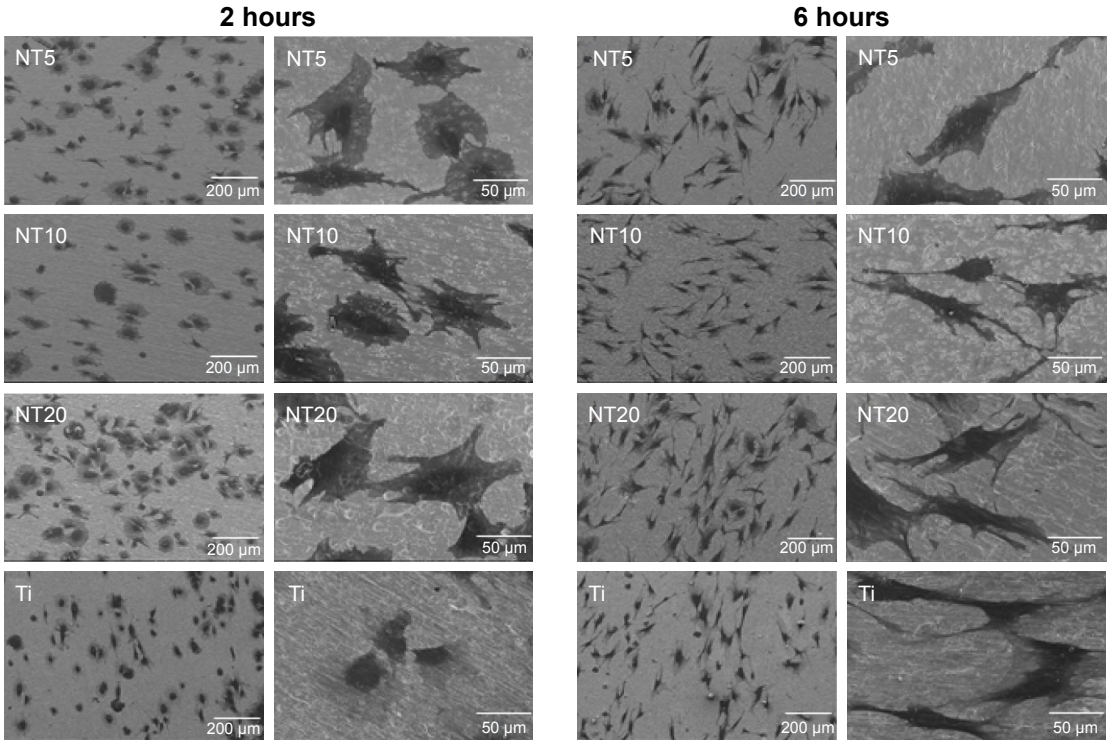

Figure 4 SEM pictures showing the morphology of cells after the first 2 and 6 hours of culture on the Ti samples.
Notes: The pictures with a low magnification of 100× (the left column) show the overall view. The pictures of 500× (the right column) show the morphology of single cells.
Abbreviations: NT, nanotube; SEM, scanning electron microscopy; Ti, titanium.

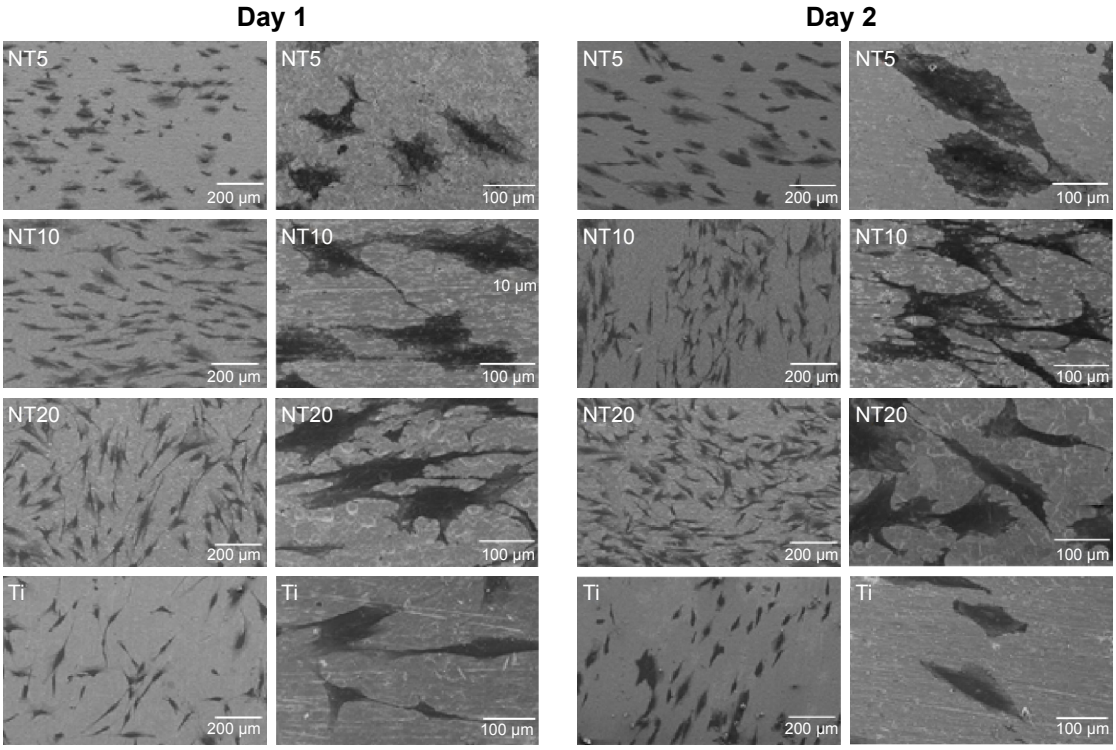

Figure 5 SEM pictures showing the morphology of cells after 1 and 2 days of culture on the Ti samples.
Notes: The pictures with a low magnification of 100× (the left column) show the overall view. The pictures of 500× (the right column) show the morphology of single cells, with the inset showing much higher magnification ones.
Abbreviations: NT, nanotube; SEM, scanning electron microscopy; Ti, titanium.

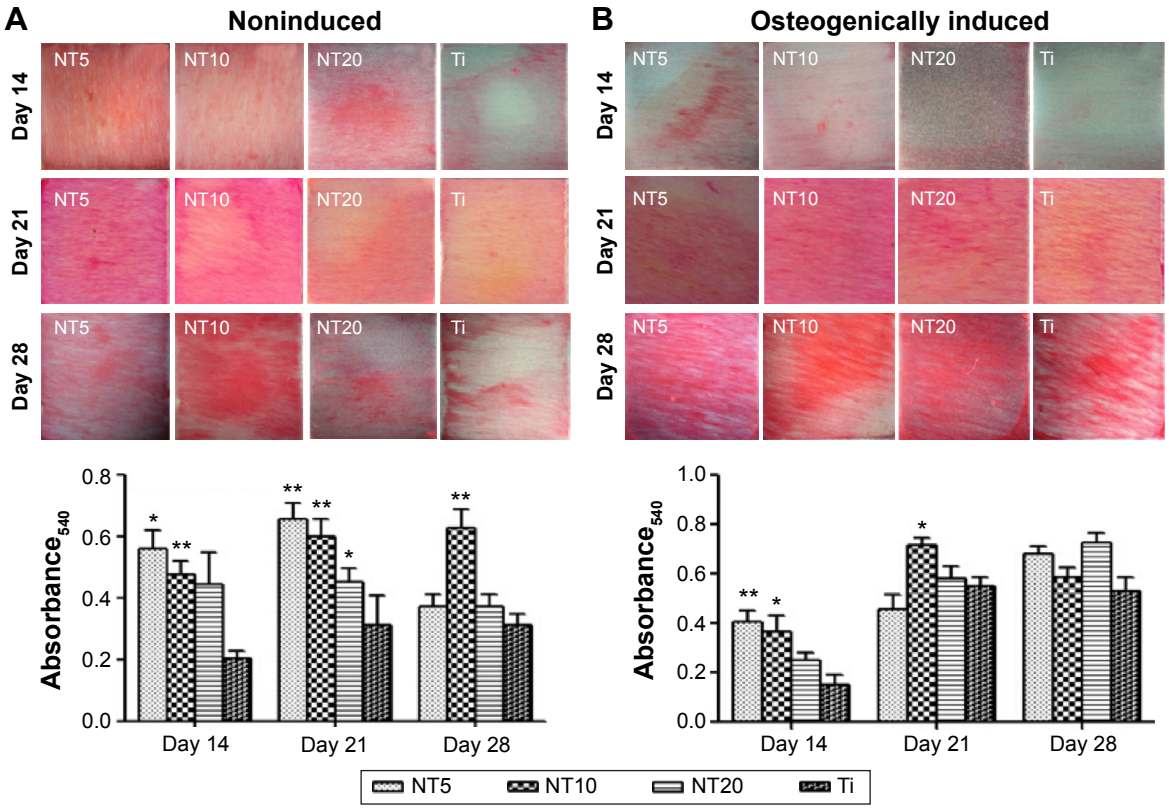

Figure 6 Collagen secreted by the PDLSCs on the different samples after 14, 21, and 28 days of incubation in the (**A**) absence and (**B**) presence of osteogenic supplements.
Notes: The upper panels list the optical images, and the lower panels show the quantitative colorimetric results. *$P<0.05$, and **$P<0.01$ compared with the Ti control.
Abbreviations: NT, nanotube; PDLSC, periodontal ligament stem cell; Ti, titanium.

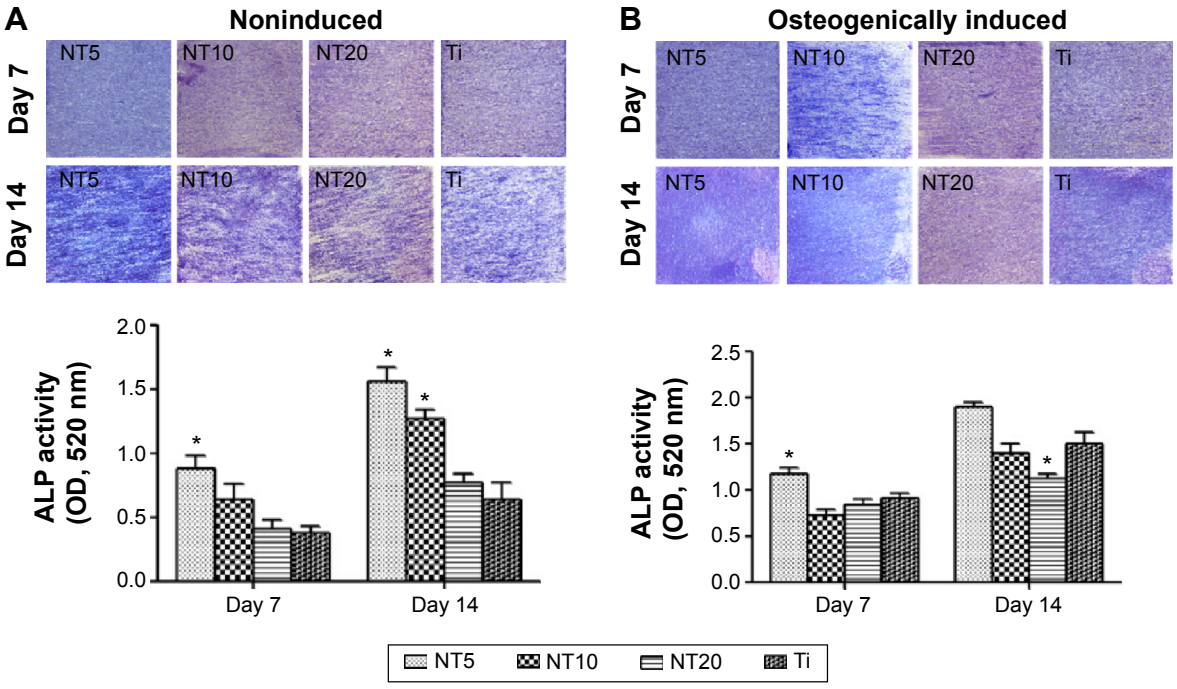

Figure 7 ALP production by the PDLSCs on the different samples after (**A**) 7 and (**B**) 14 days of incubation in the absence and presence of osteogenic supplements, as assessed by the ALP staining and ALP activity assay. *$P<0.05$ compared with the Ti control.
Abbreviations: ALP, alkaline phosphatase; NT, nanotube; PDLSC, periodontal ligament stem cell; Ti, titanium.

staining and activity assay results, we can see that the ALP product increased with the culture duration from day 7 to day 14. In the absence of osteogenic supplements, NT5 and NT10 induced more ALP product than did the Ti control, while NT20 showed no obvious difference. The presence of osteogenic supplements changed the trend of the ALP product among the different Ti groups. At both time slots, NT5 generated higher ALP product than did the other three Ti samples.

The ECM mineralization ability of the PDLSCs on the Ti samples

The ECM mineralization ability of the PDLSCs was assessed after 4 weeks of incubation, in the absence and presence of osteogenic supplements, by the Alizarin Red S staining (Figure 8). We found that the PDLSCs showed no mineralization ability in the absence of osteogenic supplements. In the presence of osteogenic supplements, the PDLSCs generated mineralized nodules. Compared with the Ti control, NT10 showed similar mineralization-inducing ability, but NT5 and NT20 displayed a lower ability.

The gene expression of the PDLSCs cultured on the Ti samples as well as the in vitro cultured Ti/cell sheets/HA complexes

The expression of genes, including COL-I, COL-III, S100A4, POSTN, and ALP, by the PDLSCs and the in vitro cultured

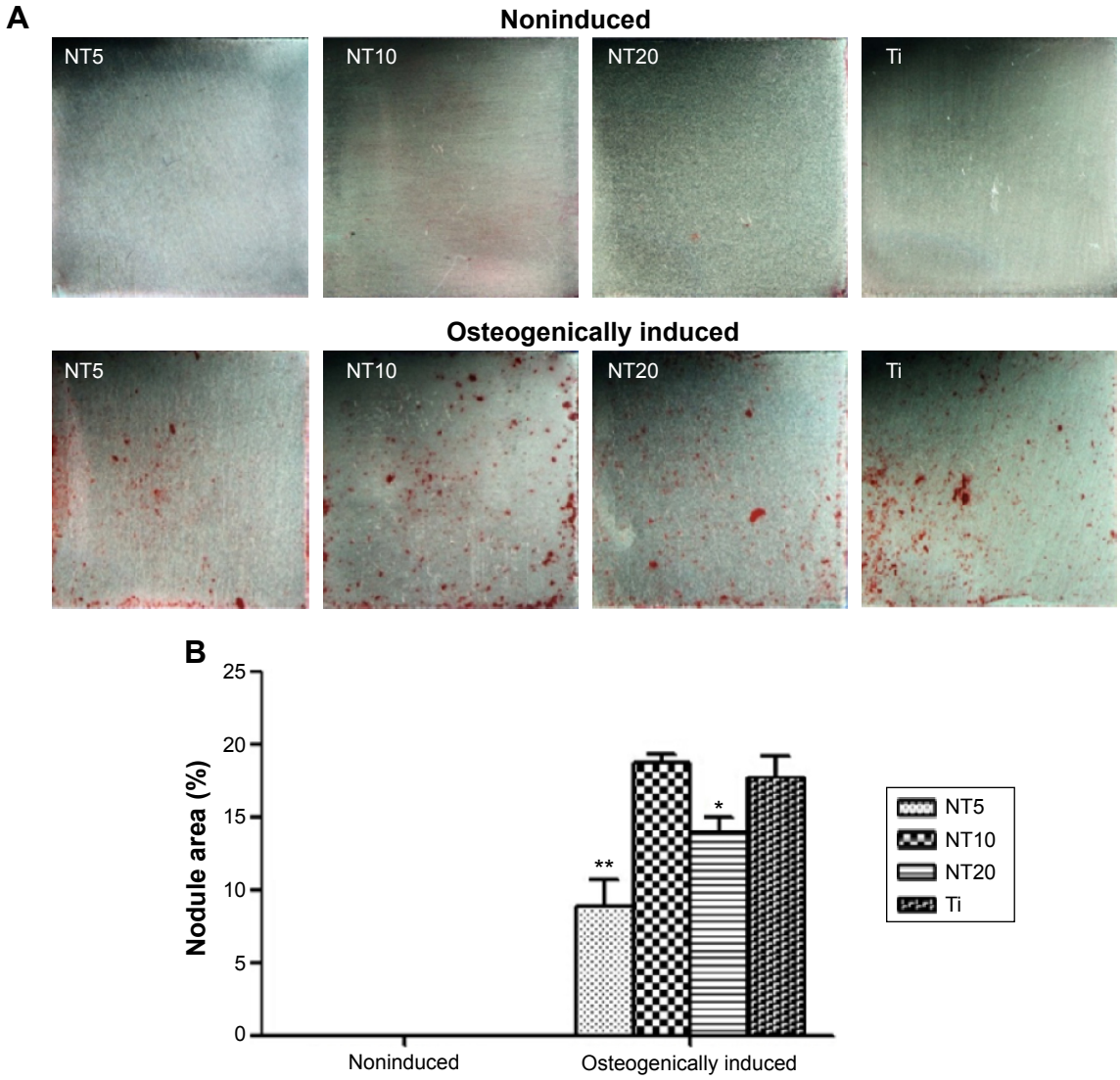

Figure 8 ECM mineralization on the different samples after 4 weeks incubation of the PDLSCs in the absence and presence of osteogenic supplements. (**A**) The optical images and (**B**) the quantitative results.
Notes: *$P<0.05$, **$P<0.01$ compared with the Ti control.
Abbreviations: ECM, extracellular matrix; NT, nanotube; PDLSC, periodontal ligament stem cell; Ti, titanium.

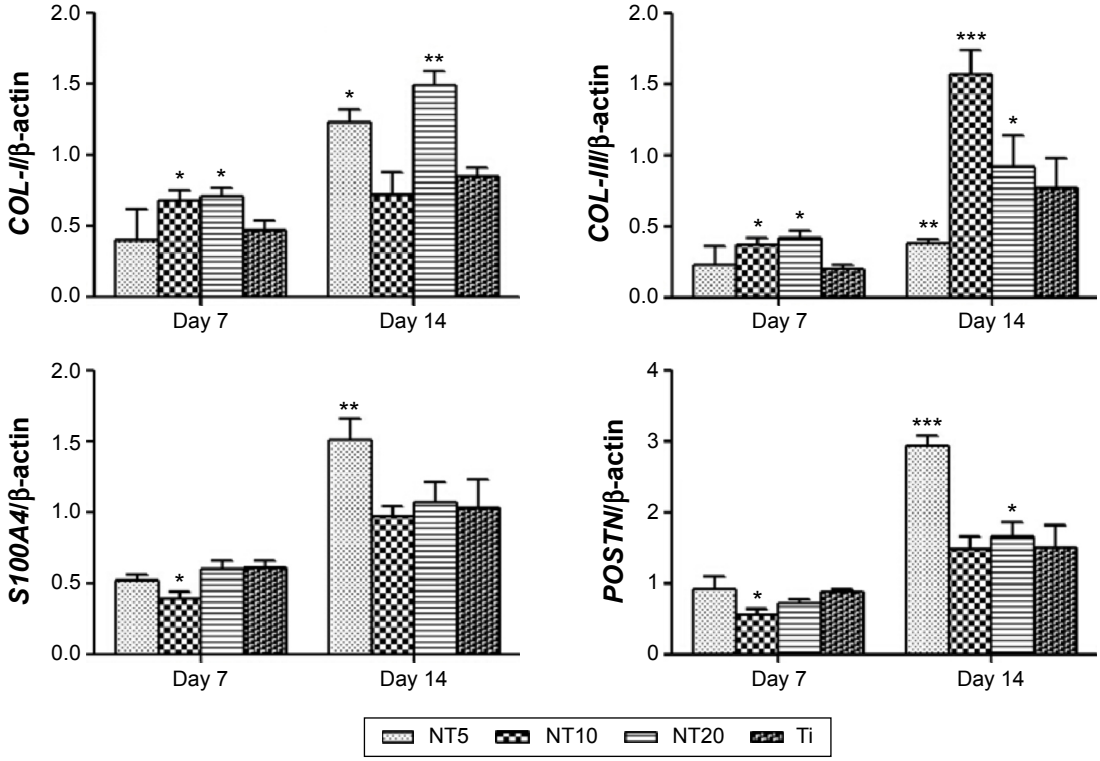

Figure 9 Expression of *COL-I*, *COL-III*, *S100A4*, and *POSTN* of the PDLSCs, after 1 and 2 weeks of culture, on the different Ti samples in the absence of osteogenic supplements, as measured by qRT-PCR.
Notes: *$P<0.05$, **$P<0.01$, and ***$P<0.001$ compared with the Ti control.
Abbreviations: NT, nanotube; PDLSC, periodontal ligament stem cell; qRT-PCR, quantitative reverse-transcription polymerase chain reaction; Ti, titanium.

Ti/cell sheets/HA complexes were assessed by qRT-PCR (Figures 9 and 10). For the PDLSCs cultured on the Ti surfaces, generally the expression of the genes increased with time from day 7 to day 14. For COL-I, compared with the Ti control, NT10 and NT20 induced higher expression at day 7, and NT5 and NT10 induced higher expression at day 14. For COL-III, NT10 and NT20 induced higher expression at both time slots, and NT5 induced lower expression at day 14. For S100A4, NT10 induced slightly lower expression at day 7, and NT5 induced higher expression at day 14; the trend for POSTN expression was similar to that of S100A4.

The expression of the genes by the Ti/cell sheets/HA complexes was measured after 1 month of in vitro culture. NT5 and NT10 induced higher expression of COL-I than did the Ti control. For COL-III, NT10 induced higher expression, but NT5 induced lower expression. For S100A4 and POSTN, all the three NT samples generated much higher expression.

In vivo ectopic PDL regeneration

At 8 weeks after the subcutaneous transplantation of the Ti/cell sheets/HA complexes in mice, the Ti/cell sheets/HA interfaces were analyzed after slicing the hard tissue and staining with Van-Gieson stain. The results obtained from the animals of respective groups were consistent, with the representative picture shown in Figure 11. Generally, there were collagen fiber bundles formed between Ti and HA in all the four groups, indicating that the Ti/cell sheets/HA complex is a good in vivo ectopic periodontal regeneration strategy to stimulate PDL-like tissue regeneration. In the Ti control group, there were relatively loose collagen fibers formed, which aligned mainly parallel to the surfaces of Ti and HA, indicating a relatively poor periodontal regeneration. On contrary, the NTs gave rise to typically disposed, dense collagen fiber bundles with abundant blood vessels formed between them. In particular, in the groups of NT10 and NT5, a layer of cementum-like tissue was observed on the Ti surfaces. Compared with NT20, NT5, and NT10 generated much denser collagen fibers and more blood vessels. The PDL-like tissues regenerated by NT5 and NT10 more closely resembled the physiological structure of natural PDL tissue.

Discussion

Periodontal regeneration is an important field in regenerative medicine and is of high clinical significance. Uncovering the factors that can influence the periodontal regeneration process

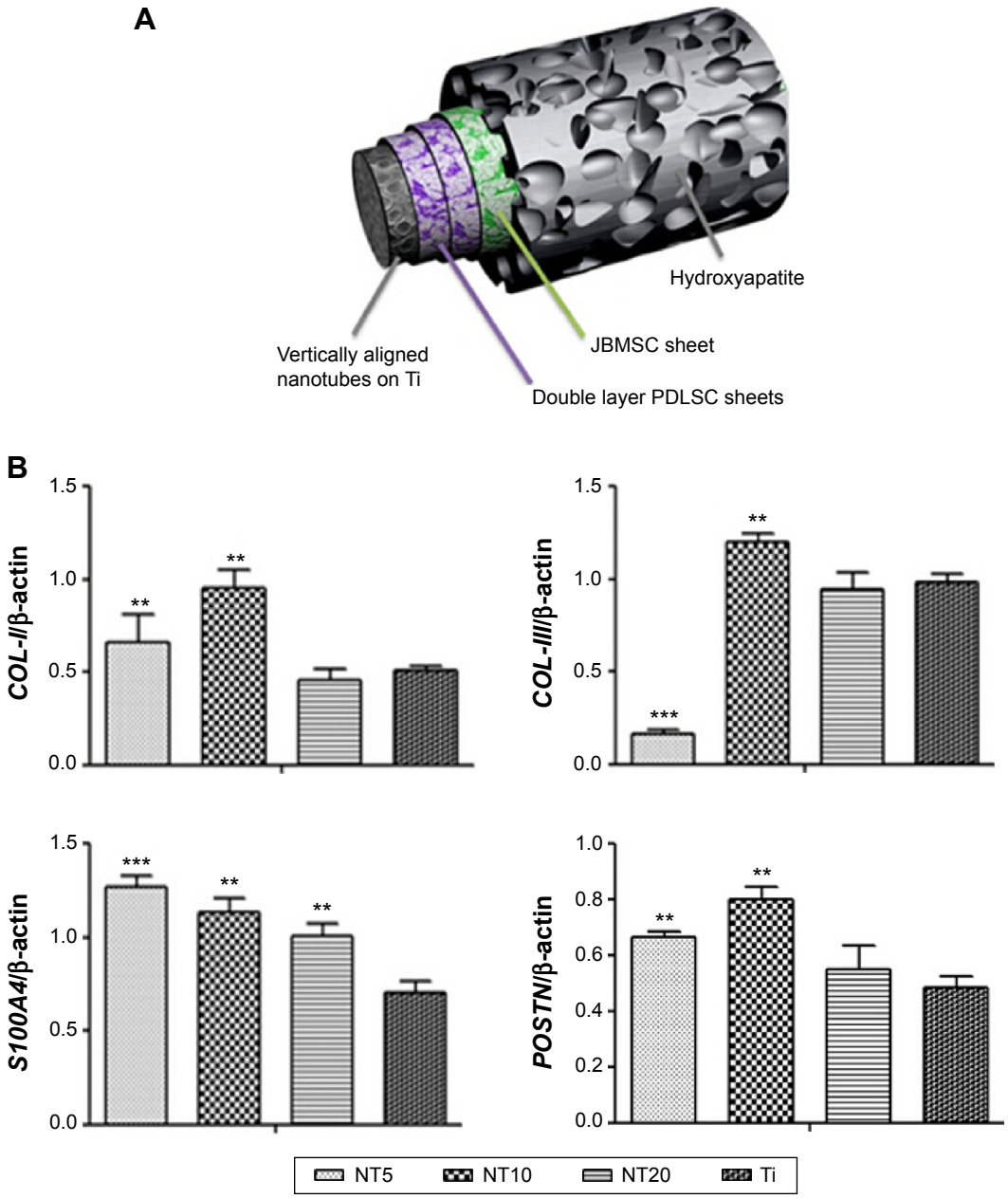

Figure 10 (**A**) The schematics showing the structure of the Ti/cell sheets/HA complex. (**B**) Expression of *COL-I*, *COL-III*, *S100A4*, and *POSTN* by the cell sheets in the Ti/cell sheets/HA complexes after 1 month of in vitro culture in the absence of osteogenic supplements, as measured by qRT-PCR.
Notes: $^{**}P<0.01$ and $^{***}P<0.001$ compared with the Ti control.
Abbreviations: HA, hydroxyapatite; JBMSC, jaw bone marrow mesenchymal stem cell; NT, nanotube; PDLSC, periodontal ligament stem cell; qRT-PCR, quantitative reverse-transcription polymerase chain reaction; Ti, titanium.

is essential to accomplish the ideal periodontal regeneration outcome. The fate of a cell can be modulated by a variety of signals, including soluble chemical cues, biomechanical cues, as well as by biophysical cues from the ECM.[22] Even though the effects of soluble chemical and biomechanical cues on the functions of PDLSCs as well as their periodontal tissue-regeneration ability have been extensively studied,[23] the influence of biophysical cues, including nanotopography, has rarely been concerned. The data obtained from some other stem cell types, such as BMSCs and embryonic stem cells, have explicitly demonstrated the robust role of nanotopography on cell fate manipulation,[17,24] which greatly encourages us to consider the potential role of nanotopography in the periodontal regeneration ability of PDLSCs. Among the different kinds of nanotopographies reported, NTs that can be fabricated with precisely controlled diameters and lengths have generated considerable interest in controlling the stem cell fate and constitute a good platform for study of the role of

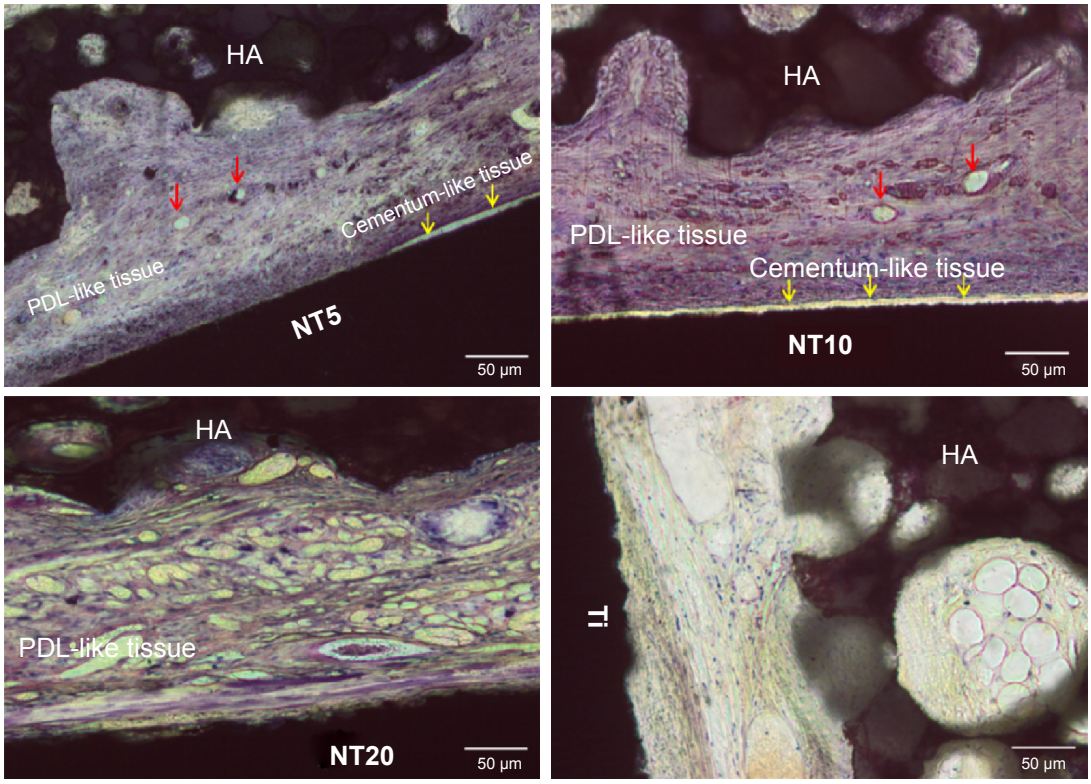

Figure 11 The Ti/cell sheets/HA interfaces analyzed by the hard tissue slicing and Van Gieson staining 8 weeks after the subcutaneous transplantation of the Ti/cell sheets/HA complexes in mice. The red arrows indicate the blood vessels, and the yellow arrows indicate the regenerated cementum-like tissue.
Abbreviations: HA, hydroxyapatite; NT, nanotube; PDL, periodontal ligament; Ti, titanium.

nanotopography in PDLSC functions.[16,17] Our results display that the NTs can enhance the initial PDLSC adhesion and spread as well as collagen secretion. By applying the Ti/cell sheets/HA complex model, it was demonstrated that the NTs could improve the periodontal regeneration result, giving rise to PDL-like dense collagen fiber bundles. In particular, abundant blood vessels, as well as a layer of cementum-like tissue on the Ti surfaces, were regenerated by the NT5 and NT10 samples. Our data, for the first time, explicitly demonstrates the obvious effects of nanotopographical cues in manipulating PDLSC functions as well as PDLSC sheet based periodontal regeneration.

The initial adhesion of anchorage-dependent cells is a pivotal process for their subsequent function.[25] Here, an enhanced initial PDLSC adhesion by the NTs was observed, and NT20 gave rise to the largest initial adherent cell number, which was related to the better cell spread on the NTs, especially NT20, as shown in Figure 4. Good spread indicates potential high cellular attachment strength to the substrate and thus high initial adherent cell number. The data obtained from the PDLSCs are inconsistent from those obtained from other cell types. Our previous observations of osteoblasts[19] and BMSCs[17] showed no obvious difference in the initial adherent cell numbers on the NTs compared with the Ti control. The inconsistent initial cell adhesion data obtained from PDLSCs to those from other cell types may be reasonably explained by the phenotypical difference. Hitherto, there have been plenty of data obtained from primary osteoblasts,[19] osteoblast cell lines,[15,26] endothelial cells,[27] and vascular smooth muscle cells,[27] supporting that the cells of different phenotypes respond differently to the same nanotopography. Afterward, the attachment and spread of the PDLSCs during the first 2 and 6 hours of cell/substrate interaction were inspected. At 2 hours, the cells were still not completely spread, and it was obvious that the NTs induced an obviously larger cell area, demonstrating that the NTs can provoke a much quicker cell spread process. After 6 hours of incubation, the cells had already spread well to mainly assume a spindle-shape with abundant long lamellipodia. Relatively longer culture durations of 1 and 2 days displayed that the beneficial cell spread effect of the NTs was long-lasting. The promoting effect of the NTs on PDLSC spread is in good accordance with the previous report that NTs enhanced the spread of BMSCs.[17] We know that the shape of stem cells on biomaterials is closely related to their fate. For BMSCs, the well-spread ones are believed to undergo osteogenesis, and

the poorly spread ones will differentiate into adipocytes.[28–30] For PDLSCs, what the shape means to their fate is still unclear and in need of deeper study.

The cell cycle analytical results suggest that NT5 and NT10 had a slightly supportive effect on the cell cycle propagation of the PDLSCs, while the cell proliferation assay results demonstrate that there were equal or slightly smaller cell numbers with the NTs than the Ti control. This phenomenon may be explained by the reciprocal relationship between cell proliferation and differentiation.[31] Even though the NTs could improve PDLSC mitosis, the differentiation tendency of the PDLSCs on the NTs finally led to equal or slightly smaller cell numbers. In addition, when undergoing cellular division, the cells need to detach slightly from the substrate, and too tight adhesion may hinder the cell division process. Thus, the greatly improved cell extension and their close attachment to the NT surfaces, as disclosed by the FE-SEM pictures in Figures 4 and 5, physically hindered the cell division process, thus partially contributing to the equal or slightly smaller cell numbers on the NTs.

The main components of PDL are collagen fibers as well as many other ECM components, hence the ECM synthesis and secretion ability of the PDLSCs is important for regeneration of the PDL fibers. Excitingly, we observed that the NTs significantly improved the collagen secretion of the PDLSCs. Actually, in our previous studies, we also observed that NTs significantly improved the collagen secretion of BMSCs,[17] primary osteoblasts,[18,20] as well as osteoblast cell lines.[32] The collagen secretion results observed from the different cell types are consistent and support that the NTs have a general improving effect on collagen secretion in different cells. The collagen secretion results were to great extent further corroborated by the gene expression analysis. A cumulative higher COL-I and COL-III expression by the PDLSCs as well as the cells in the Ti/cell sheets/HA complex was induced by the NTs, though not all the NT samples generated enhanced collagen expression at all the time points. The enhancing effect of the NTs on cell collagen secretion is extremely meaningful for the regeneration of the periodontal tissue, where the PDL is mainly composed of collagen fibers, and the main ECM components of alveolar bone and root cementum are also collagen.

The NTs did not induce the osteogenic differentiation of the PDLSCs, as indicated by the fact that no mineralization was observed in the absence of osteogenic supplements. Only in the presence of osteogenic supplements did the mineralization occur. Even though there is still no definitive marker specific to PDL cells, POSTN and S100A4 have been relatively widely used as the specific markers for PDL cells in previous study.[33] POSTN is essential for tissue integrity and maturation and is believed to have a key function as a modulator of PDL homeostasis.[34] In human PDL, POSTN is specifically and intensely localized on Sharpey's fibers.[35] As a member of the S100 calcium-binding protein family,[36] S100A4 has been reported to be much more highly expressed in the PDL compared with other oral tissues, such as dental follicle, dental papilla, and gingiva.[37] Hence, POSTN and S100A4 were considered to be the specific markers for PDL in the present study. For the PDLSCs cultured on the Ti surfaces, NT5 induced higher expression of POSTN and S100A4, but NT10 and NT20 did not. While for the in vitro–cultured Ti/cell sheets/HA complexes, all three NT samples generated much higher expression of S100A4 and POSTN. The results indicate that the NTs effectively promoted the differentiation of the PDLSC sheets into PDL cells.

Hitherto, nearly all the periodontal regeneration trials were conducted around the natural dentin slice, since it was believed that the soluble chemical cues contained within the dentin are essential for periodontal regeneration. There have been several attempts to bioengineer a periodontal-like tissue surrounding the Ti implant, which have been mainly conducted in the alveolar bone.[38,39,40] Here, by using an ectopic implantation model of Ti/cell sheets/HA complex, where neither extra soluble chemical cues nor the periodontal tissue development niche was provided, we obviously demonstrated that the PDLSC sheets were capable of regenerating the PDL tissue, when combined with a BMSC sheet and HA. After ectopic implantation, the Ti/cell sheets/HA complex was capable of generating PDL-like collagen fiber bundles between the Ti and HA. Furthermore, it is hard to form nanotopography on the dentin slice, but various nanotopographies can be easily fabricated on Ti. Accordingly, the Ti-based PDL regeneration model provides an excellent platform to study the role of nanotopography on periodontal regeneration. Using this model, excitingly, we found that the NTs improved the periodontal regeneration results of the Ti/cell sheets/HA complex after ectopic implantation, leading to dense collagen fiber bundles. In particular, abundant blood vessels among the collagen fibers as well as cementum-like tissue on the Ti surface were observed in the NT5 and NT10 groups. Our data provide the first evidence that the nanotopographical cue obviously influences periodontal regeneration. For the NTs, there was a size-dependent effect, such that NT5 and NT10 did better than NT20, and the underlying mechanism necessitates further inspection. In future study, it will be of interest to observe the effect of other kinds of nanotopographies,

such as nanogrooves, nanopits, and nanowires, on the periodontal regeneration process. Also it will be meaningful to uncover the molecular mechanism underlying the influence of nanotopography on the periodontal regeneration process, to theoretically guide the design of the periodontal regeneration strategy.

It is noted that regarding the influence of NTs of different diameter, there was great disparity between the in vivo PDL-like tissue regeneration by the Ti/cell sheets/HA complex and the in vitro functions of isolated PDLSCs. This can be attributed the fact that the PDL tissue is a very complex structure, comprising alveolar bone, PDL, and cementum, whose regeneration cannot be resembled by the simple model of an in vitro isolated PDLSC culture. Instead, the Ti/cell sheets/HA complex proposed here should be a better model to predict the effect of biomaterials on periodontal regeneration.

Conclusion

The influence of nanotopography on the functions of PDLSCs as well as on PDLSC sheet based periodontal regeneration was observed. NTs enhanced the initial PDLSC adhesion, spread, as well as collagen secretion. Using the ectopically implanted Ti/cell sheets/HA complex model, the PDLSC sheets were able to regenerate the PDL tissue without requiring extra soluble chemical cues. The NTs improved the periodontal regeneration result, leading to the formation of collagen fiber bundles. The data obviously demonstrated that the effect of nanotopographical cues can influence the functions of PDLSCs as well as PDLSC sheet based periodontal regeneration. In addition, the Ti/cell sheets/HA complex may constitute a good model to predict the effect of biomaterials on periodontal regeneration.

Acknowledgments

This work was supported by grants from the National Natural Science Foundation of People's Republic of China (grant numbers 31030033, 31401255, 81470710, and 31200716), the National Major Scientific Research Program of People's Republic of China (grant number 2010CB944800), the Foundation for the Author of National Excellent Doctoral Dissertation of People's Republic of China (grant number 201483), the National High Technology Research and Development Program of People's Republic of China (grant number SS2015AA020921), and the Self-Selected Topic Project of State Key Laboratory of Military Stomatology (grant number 2014ZB04). LZ Zhao also appreciates the grant from the School of Stomatology, The Fourth Military Medical University.

Disclosure

The authors report no conflicts of interest in this work.

References

1. Villar CC, Cochran DL. Regeneration of periodontal tissues: guided tissue regeneration. *Dent Clin North Am*. 2010;54(1):73–92.
2. Pihlstrom BL, Michalowicz BS, Johnson NW. Periodontal diseases. *Lancet*. 2005;366(9499):1809–1820.
3. Needleman IG, Worthington HV, Giedrys-Leeper E, Tucker RJ. Guided tissue regeneration for periodontal infra-bony defects. *Cochrane Database Syst Rev*. 2006CD001724.
4. Tobita M, Uysal CA, Guo X, Hyakusoku H, Mizuno H. Periodontal tissue regeneration by combined implantation of adipose tissue-derived stem cells and platelet-rich plasma in a canine model. *Cytotherapy*. 2013; 15(12):1517–1526.
5. Tucker AS, Fraser GJ. Evolution and developmental diversity of tooth regeneration. *Semin Cell Dev Biol*. 2014;25–26:71–80.
6. Snead ML. Whole-tooth regeneration: it takes a village of scientists, clinicians, and patients. *J Dent Educ*. 2008;72(8):903–911.
7. Goriainov V, Cook R, M Latham J, G Dunlop D, Oreffo RO. Bone and metal: an orthopaedic perspective on osseointegration of metals. *Acta Biomater*. 2014;10(10):4043–4057.
8. Lamas PJ, Penarrocha DM, Marti BE, et al. Intraoperative complications during oral implantology. *Med Oral Patol Oral Cir Bucal*. 2008; 13:E239–E243.
9. Sennerby L, Ericson LE, Thomsen P, et al. Structure of the bone-titanium interface in retrieved clinical oral implants. *Clin Oral Implants Res*. 1991;2:103–111.
10. Seo BM, Miura M, Gronthos S, et al. Investigation of multipotent postnatal stem cells from human periodontal ligament. *Lancet*. 2004; 364(9429):149–155.
11. Dan H, Vaquette C, Fisher AG, et al. The influence of cellular source on periodontal regeneration using calcium phosphate coated polycaprolactone scaffold supported cell sheets. *Biomaterials*. 2014;35(1): 113–122.
12. Tsumanuma Y, Iwata T, Washio K, et al. Comparison of different tissue-derived stem cell sheets for periodontal regeneration in a canine 1-wall defect model. *Biomaterials*. 2011;32(25):5819–5825.
13. Dalby MJ, Gadegaard N, Tare R, et al. The control of human mesenchymal cell differentiation using nanoscale symmetry and disorder. *Nat Mater*. 2007;6(12):997–1003.
14. McMurray RJ, Gadegaard N, Tsimbouri PM, et al. Nanoscale surfaces for the long-term maintenance of mesenchymal stem cell phenotype and multipotency. *Nat Mater*. 2011;10(8):637–644.
15. Brammer KS, Oh S, Cobb CJ, Bjursten LM, van der Heyde H, Jin S. Improved bone-forming functionality on diameter-controlled TiO(2) nanotube surface. *Acta Biomater*. 2009;5(8):3215–3223.
16. Oh S, Brammer KS, Li YS, et al. Stem cell fate dictated solely by altered nanotube dimension. *Proc Natl Acad Sci U S A*. 2009;106(7): 2130–2135.
17. Zhao L, Liu L, Wu Z, Zhang Y, Chu PK. Effects of micropitted/nanotubular titania topographies on bone mesenchymal stem cell osteogenic differentiation. *Biomaterials*. 2012;33(9):2629–2641.
18. Zhao L, Mei S, Chu PK, Zhang Y, Wu Z. The influence of hierarchical hybrid micro/nano-textured titanium surface with titania nanotubes on osteoblast functions. *Biomaterials*. 2010;31(19):5072–5082.
19. Zhao L, Mei S, Wang W, Chu PK, Zhang Y, Wu Z. Suppressed primary osteoblast functions on nanoporous titania surface. *J Biomed Mater Res A*.2011; 96(1):100–107.
20. Zhao L, Mei S, Wang W, Chu PK, Wu Z, Zhang Y. The role of sterilization in the cytocompatibility of titania nanotubes. *Biomaterials*. 2010; 31(8):2055–2063.
21. Iwata T, Yamato M, Tsuchioka H, et al. Periodontal regeneration with multi-layered periodontal ligament-derived cell sheets in a canine model. *Biomaterials*. 2009;30(14):2716–2723.
22. Discher DE, Mooney DJ, Zandstra PW. Growth factors, matrices, and forces combine and control stem cells. *Science*. 2009;324(5935):1673–1677.

23. Gao LN, An Y, Lei M, et al. The effect of the coumarin-like derivative osthole on the osteogenic properties of human periodontal ligament and jaw bone marrow mesenchymal stem cell sheets. *Biomaterials*. 2013;34(38):9937–9951.
24. Ankam S, Suryana M, Chan LY, et al. Substrate topography and size determine the fate of human embryonic stem cells to neuronal or glial lineage. *Acta Biomater*. 2013;9(1):4535–4545.
25. Anselme K. Osteoblast adhesion on biomaterials. *Biomaterials*. 2000; 21(7):667–681.
26. Popat KC, Eltgroth M, Latempa TJ, Grimes CA, Desai TA. Decreased Staphylococcus epidermis adhesion and increased osteoblast functionality on antibiotic-loaded titania nanotubes. *Biomaterials*. 2007; 28(32):4880–4888.
27. Peng L, Eltgroth ML, LaTempa TJ, Grimes CA, Desai TA. The effect of TiO2 nanotubes on endothelial function and smooth muscle proliferation. *Biomaterials*. 2009;30(7):1268–1272.
28. McBeath R, Pirone DM, Nelson CM, Bhadriraju K, Chen CS. Cell shape, cytoskeletal tension, and RhoA regulate stem cell lineage commitment. *Dev Cell*. 2004;6(4):483–495.
29. Kilian KA, Bugarija B, Lahn BT, Mrksich M. Geometric cues for directing the differentiation of mesenchymal stem cells. *Proc Natl Acad Sci U S A*. 2010;107(11):4872–4877.
30. Peng R, Yao X, Ding J. Effect of cell anisotropy on differentiation of stem cells on micropatterned surfaces through the controlled single cell adhesion. *Biomaterials*. 2011;32(32):8048–8057.
31. Stein GS, Lian JB, Owen TA. Relationship of cell growth to the regulation of tissue-specific gene expression during osteoblast differentiation. *FASEB J*. 1990;4(13):3111–3123.
32. Wang W, Zhao L, Ma Q, Wang Q, Chu PK, Zhang Y. The role of the Wnt/β-catenin pathway in the effect of implant topography on MG63 differentiation. *Biomaterials*. 2012;33(32):7993–8002.
33. Chen K, Xiong H, Huang Y, Liu C. Comparative analysis of in vitro periodontal characteristics of stem cells from apical papilla (SCAP) and periodontal ligament stem cells (PDLSCs). *Arch Oral Biol*. 2013; 58(8):997–1006.
34. Padial-Molina M, Volk SL, Rodriguez JC, Marchesan JT, Galindo-Moreno P, Rios HF. Tumor necrosis factor-α and Porphyromonas gingivalis lipopolysaccharides decrease periostin in human periodontal ligament fibroblasts. *J Periodontol*. 2013;84(5):694–703.
35. Kashima TG, Nishiyama T, Shimazu K, et al. Periostin, a novel marker of intramembranous ossification, is expressed in fibrous dysplasia and in c-Fos-overexpressing bone lesions. *Hum Pathol*. 2009;40(2): 226–237.
36. Schäfer BW, Wicki R, Engelkamp D, Mattei MG, Heizmann CW. Isolation of a YAC clone covering a cluster of nine S100 genes on human chromosome 1q21: rationale for a new nomenclature of the S100 calcium-binding protein family. *Genomics*. 1995;25(3):638–643.
37. Duarte WR, Kasugai S, Iimura T, et al. cDNA cloning of S100 calcium-binding proteins from bovine periodontal ligament and their expression in oral tissues. *J Dent Res*. 1998;77(9):1694–1699.
38. Oshima M, Inoue K, Nakajima K, et al. Functional tooth restoration by next-generation bio-hybrid implant as a bio-hybrid artificial organ replacement therapy. *Sci Rep*. 2014;4:6044.
39. Park JC, Oh SY, Lee JS, et al. In vivo bone formation by human alveolar-bone-derived mesenchymal stem cells obtained during implant osteotomy using biphasic calcium phosphate ceramics or Bio-Oss as carriers. *J Biomed Mater Res B Appl Biomater*. Epub 2015 May 1.
40. Pilipchuk SP, Plonka AB, Monje A, et al. Tissue engineering for bone regeneration and osseointegration in the oral cavity. *Dent Mater*. 2015;31(4):317–338.

Supplementary materials

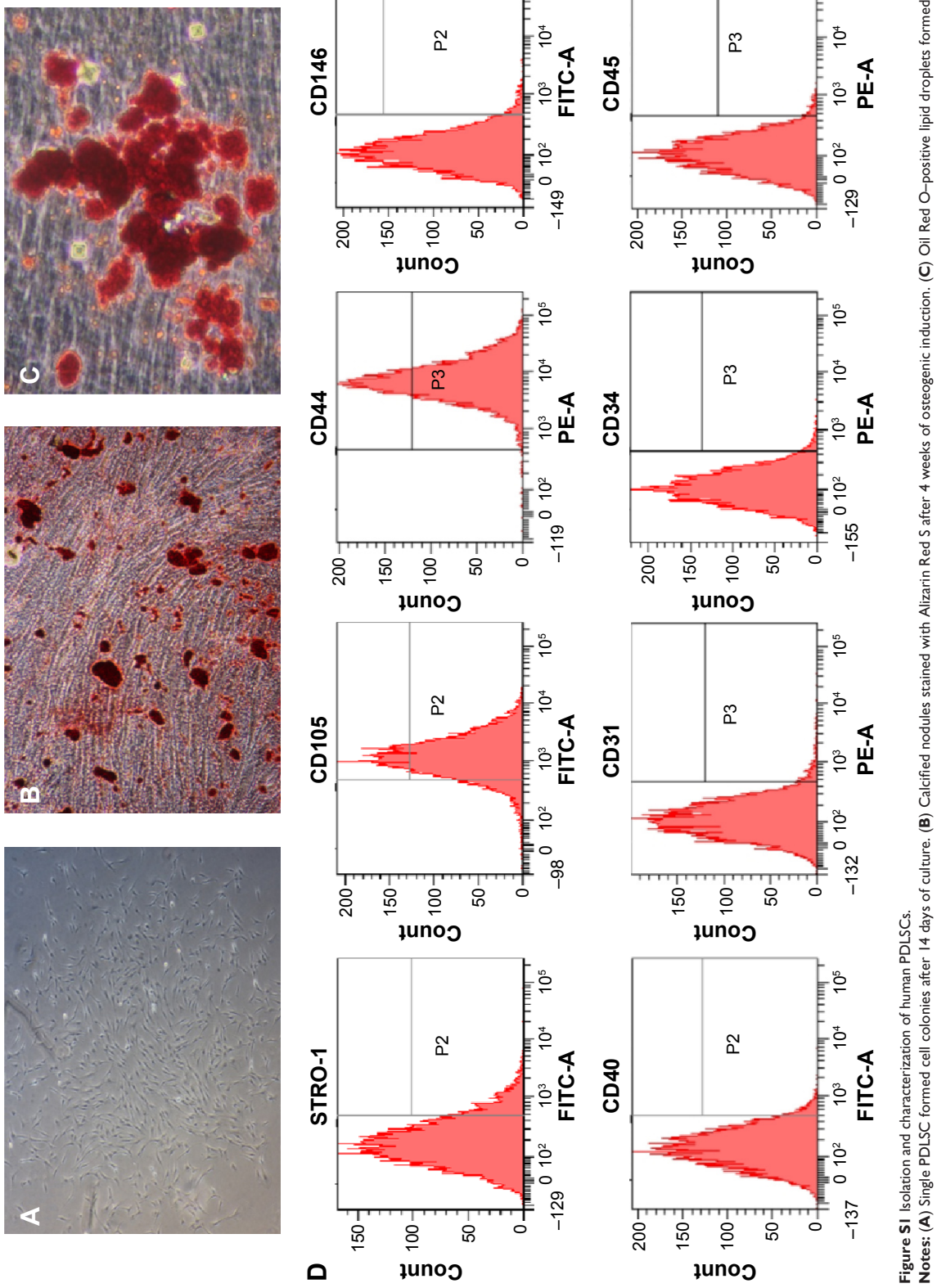

Figure S1 Isolation and characterization of human PDLSCs.
Notes: (**A**) Single PDLSC formed cell colonies after 14 days of culture. (**B**) Calcified nodules stained with Alizarin Red S after 4 weeks of osteogenic induction. (**C**) Oil Red O–positive lipid droplets formed after 3 weeks of adipogenic induction. (**D**) Flow cytometry analysis on the surface markers of PDLSCs.
Abbreviation: PDLSC, periodontal ligament stem cell.

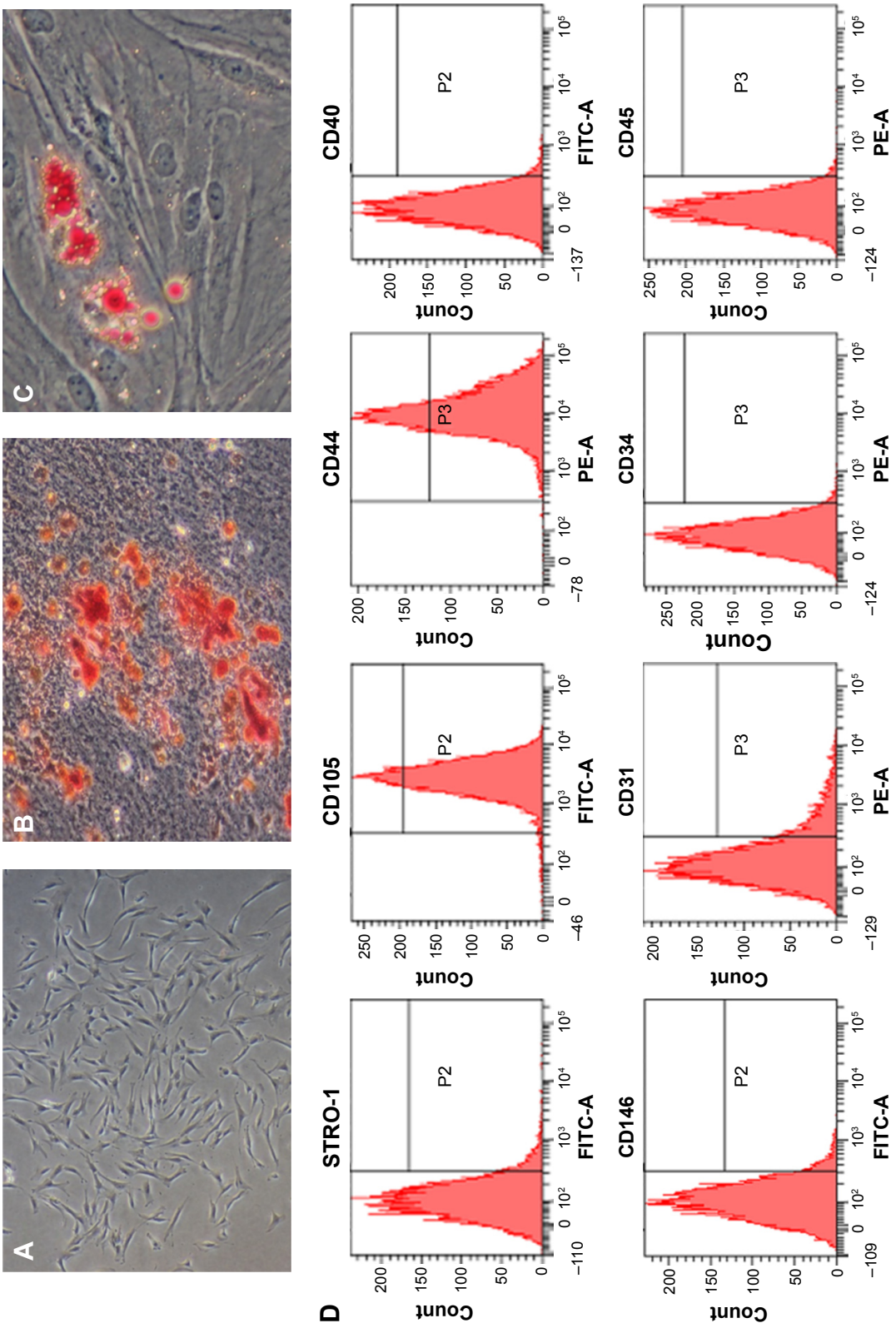

Figure S2 Isolation and characterization of human BMSCs.
Notes: (**A**) Single BMSC formed cell colonies after 14 days of culture. (**B**) Calcified nodules stained with Alizarin Red S after 4 weeks of osteogenic induction. (**C**) Oil Red O–positive lipid droplets formed after 3 weeks of adipogenic induction; (**D**) Flow cytometry analysis on the surface markers of BMSCs.
Abbreviation: BMSC, bone marrow mesenchymal stem cell.

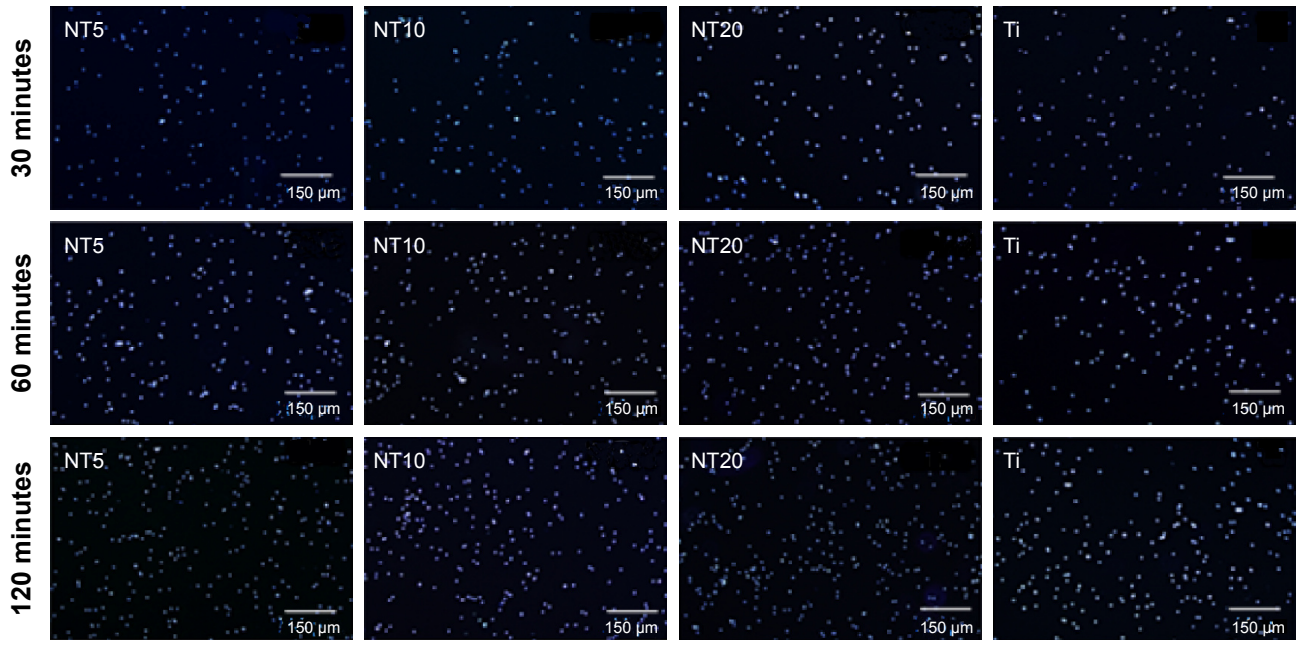

Figure S3 The initial PDLSC adhesion on the Ti samples displayed by DAPI-staining followed by observation under the fluorescence microscopy, after 30, 60, and 120 minutes of incubation.
Note: Scale bars are 150 μm.
Abbreviations: DAPI, 4′,6′-diamidino-2-phenylindole; PDLSC, periodontal ligament stem cell; Ti, titanium.